Initial states of core flooding techniques evaluation: a global pore-scale investigation

Franck Nono[1,*], *Cyril* Caubit[2], and *Richard* Rivenq[2]

[1]Modis, Pau, France
[2]TotalEnergies, Pau, France

Abstract. Initial water saturation (S_{wi}) preceding waterflooding experiments is an important factor because it impacts multiphase flow properties and the degree of wettability reached after ageing. There exist various techniques aiming to achieve S_{wi} on core plugs but there is scarce data which compare them and size their differences down to the pore-scale and considering wettability. The available data show large quantitative discrepancies with the best choices often not clear. In fact, already obtaining homogeneous profiles with average values comparable to reservoirs states in reasonable time is not so straightforward. Relying only on both these aspects to judge the quality of an initialization technique may hide possible pore scale artifacts.

In this work, we used 3D X-ray microtomography to compare at the pore scale different targets of S_{wi} achieved using porous-plate, viscous displacement, and centrifuge techniques. We used mini plugs from Bentheimer sandstone with different initial wettabilities. Pore-scale properties such as pore occupancy, fluids connectivity, etc., were investigated. Multiphase flow properties were also measured during tests. Our study is mainly focused on: (i) the impact of the initialization technique, (ii) the Impact of rock's initial wettability.

For water-wet plugs, all techniques exhibit similar pore-scale results for low targets of S_{wi}. In the other hand, capillary end-effects are the crucial artefacts for higher S_{wi} targets. Recirculation or reverse spinning to flatten saturation profiles generates disconnected oil clusters. The porous plate method delivered robust results. For oil-wet plugs, viscous displacement generates large brine ganglia trapped in big pores and difficult to mobilize thus leading to unwanted high S_{wi}. These observations are made despite suitable rocks permeabilities. The trends are confirmed by investigations of core cleaning efficiency. For identical primary drainage protocols before and after cleaning, we observed a repeatable increase of S_{wi} after cleaning. Nevertheless, in our experiments the after-cleaning oil-wetness was so low that brine occupied smaller pores as wanted.

These experimental observations clearly highlight the possible non-negligible impacts of primary drainage techniques, the protocols associated and the rock wettability on establishing a representative S_{wi} prior to multiphase flow experiments.

1 Introduction

In order to understand multiphase flow processes at the field scale for various important purposes (soil remediation, oil recovery, CO2 injection, etc.) flow experiments are conducted at the core scale in laboratories with conditions very close to reservoirs conditions. It implies having the same initial fluids distribution as in specific locations of the reservoir. Unfortunately, there is no direct initial pore-scale in situ observation to rely on, but it is stated that all reservoir rocks were initially water-wet before oil migration and the initial water saturation (i.e. in oil-water transition zone) or irreducible water saturation (S_{wirr}) was first located at the pores surface (films) [1], in small pores, corners and crevices. After what, an ageing process occurred through millions of years and impacted the affinity of the reservoir rock with the reservoir fluids. In laboratories, this process is then repeated prior to oil recovery experiments on smaller time scales. S_{wi} is an important parameter as it sets the departure of various flow properties measurements [2] which will depend not only on its average value but also on its distribution within the pore network. To resume, it is important to set S_{wi} alike a water wet state so for its distribution after ageing to be close to that of the reservoir, keeping in mind that there is a big assumption on the fact that the ageing time in laboratories will be able to achieve the same wettability of the reservoir that was achieved during millions of years.

From core flooding laboratory perspective, experimental investigations need a start on almost water-wet cores. To do so, drilled reservoir plugs are cleaned with specific solvents before achieving S_{wi} in order to restore the initial water-wet state [2, 3]. Nevertheless, cleaning is known to not always being efficient [4] and can lead to non-water-wet plugs prior to SCAL experiments. In these cases, wettability may play an important role on S_{wi} distribution [5]. The long-time concept of phases distribution during a non-water-wet primary drainage is always hypothesized to explain behaviours such as low effective oil permeability at S_{wi} [5]. Moreover, pore occupancy is meant to be inversed to that of a water-wet case, meaning large blobs of brine trapped in big pores and oil in small pores. There are no direct pore

* Corresponding author: franck.nono@modis.com

scale observations of this trapping on real rocks. The only experimental observations are those coming from micromodels or artificial porous media (acrylic bead packs) [6]. The authors observed significant larger brine blobs population in oil-wet bead packs than in water-wet cases with slight changes of saturation, although over one order of magnitude increase in flowrate.

The three most used techniques [3] to achieve initial water saturation on core plugs in laboratories are: (i) dynamic displacement, (ii) porous-plate and (iii) centrifuge. These methods are well documented at the macro-scale and their theoretical and practical advantages and drawbacks seem to be known. In one hand, the porous plate method generally delivers robust results and can target a wide range of S_{wi} but is time consuming. In addition, limitation of the ceramic maximum capillary pressure [4] or experimental artefacts such as poor capillary contact with rock may introduce significant errors [7] and render S_{wi} difficult to obtain. Improvements of this method are mainly focused in reducing the measurement time, by modifying the geometry and/or the intrinsic properties of the porous plate [2, 8]. In the other hand, both dynamic displacement and centrifuge methods are faster to implement but generate gradient of saturation profiles along the plug because of the capillary end-effect [9]. In these cases, plugs sometimes undergo reverse flow injection or reverse spinning [2, 10] to flatten saturation profiles. Limitations in terms of set-up limits such as maximum flowrates, maximum pressures or maximum spinning rates can emphasize the difficulty of reaching low S_{wi}, specifically when dealing with low permeable rocks [1].

In general case the main point of control for quality check of an experimental S_{wi} in comparison with that of the reservoir is its average value. For laboratories equipped with In-situ saturation monitoring (ISSM) set-ups, both the average value and homogeneous profile are the main criteria to attest for a good departing point for flooding experiments. Meanwhile large inconsistencies and discrepancies are still observed on multiphase flow properties even after achieving almost the same S_{wi} on the same rock-type, with same fluids but different initializing methods [7]. The consensus about the best method to use (fast and accurate) is not clear. Macro-scale properties seem to not be sufficient to identify the source of these discrepancies. Recent studies [11, 12] specifically compared the flooding and centrifuge techniques till the nanoscale on a dual porosity carbonate rock (Ketton limestone). It appeared that samples which went through centrifuge experiments became finally more oil-wet than samples which underwent oil flooding. The difference was ascribed to reachable level of capillary pressure and the pore network structure. During flooding, in a section brine fills the pores and throats located on the easiest path while for centrifuge all the pores and throats with radius above the applied capillary pressure radius are filled. Moreover, if the water-wet network is made of two distinct paths (micro and macro porosity) not well connected like Ketton limestone; oil flooding would likely miss the micro-porosity invasion. Nevertheless, some questions remain on how capillary end effect was considered, its impact on the results or the impact of dopants on wettability as it was used on final water-wet experiments and not used on final oil-wet experiments.

In this study, we used 3D X-ray microtomography to investigate and compare fluids dispositions at the pore scale after S_{wi} achievement using the three methods discussed above with exactly the same fluids and experimental conditions. In order to eliminate any issue related to set-up limits, we decided to work on suitable unimodal rocks enabling a large range of S_{wi} to be targeted by any method. We focused our study on two main axes:

(i) Water-wet S_{wi} comparisons at the pore scale using different initializing method: It will help us to settle thoroughly the crucial differences and point out drawbacks of some routines in primary drainage protocols

(ii) Impact of rock's initial wettability on primary drainage: This point is investigated via two different strategies: first by performing primary drainage on artificially made non-water wet outcrops and second by performing primary drainage on outcrops that were cleaned after their wettability was modified using crude oil.

2 Materials and methods

2.1. Porous media: Bentheimer sandstone

Primary drainage experiments till S_{wi} were performed on fresh cylindrical Bentheimer sandstones The mineralogy is reported in Table 1.

Table 1. Mineralogy of the rock-type used in this study

Bentheimer	96% Quartz, 3% Clays, feldspar.

Bentheimer mean pore throat diameter averages 30µm to 40µm. It is known to be homogeneous with an absolute permeability around 1 to 3 Darcy and a porosity around 20% to 25%. This outcrop is initially water wet. Experiments performed in this study also include achieving S_{wi} on Bentheimer plugs which had their initial water wettability

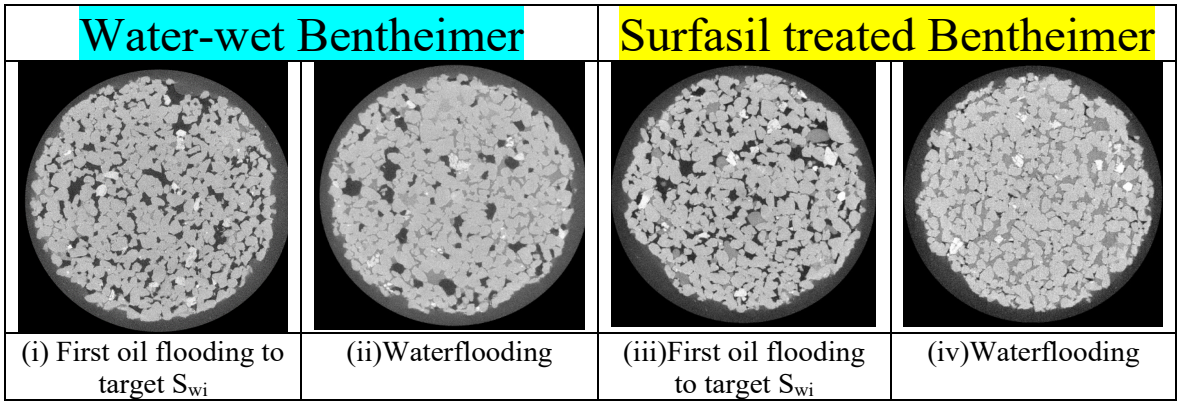

Figure 1 : Comparisons of pore-space occupancy between water-wet Bentheimer at S_{wi} (ii) and S_{or} (ii) and Surfasil treated Bentheimer at S_{wi} (iii) and S_{or} (iv).

altered. Two different procedures were used to alter Bentheimer sandstones wettability prior to flooding. For some plugs, a chemical alteration was used and consisted in saturating under vacuum the water-wet pore space with a mixture of toluene (95%) and Surfasil® (5%), directly followed with 3 min of ageing at room temperature. After that, the samples were flushed with 100% toluene, then cleaned and dried in an oven. A proof of wettability alteration through this chemical protocol is shown in figure 1. This chemical treatment tends to artificially homogenize the oil wetness behaviour of the pore space while for natural rocks, wettability may vary within the pore space. In this study, we have to think about the micro-plugs as part of larger size plugs. The goal is to focus on the impact of a well identified wettability on the trapping process. We achieved quick flooding test, coupled with 3D X-ray imaging to compare the visual differences between water-wet and altered wettability greyscale images on Bentheimer during primary drainage and waterflooding with same fluids. One can refer to Nono et al., 2019 [9], section 3.5, to understand the colour code of the greyscale reconstructed data. As we can see, oil flooding and waterflooding images between water-wet media and Surfasil-treated media are

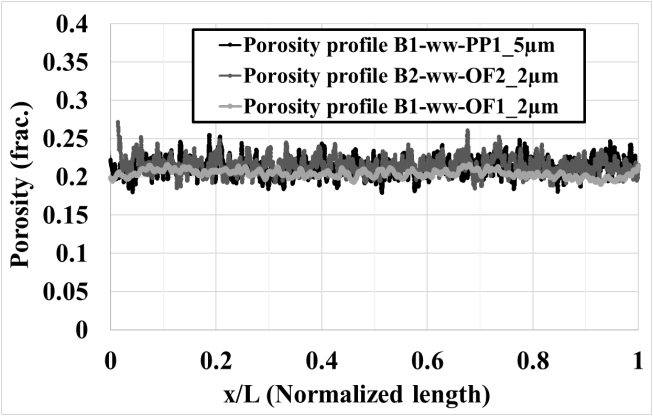

Figure 2. Examples of Bentheimer plugs porosity profiles obtained through 3D image processing.

totally different, especially the end of the waterflooding processes. We observe large blobs of oil in big pores for water-wet media (as expected), while oil remains in very small pores for Surfasil-treated media. Thus, we were confident that our Surfasil-treated media were not water-wet. For other plugs, we altered wettability by a more or less efficient cleaning that followed an ageing process (at very low S_{wi}) of 15 days with dead oil (crude oil A) at 80°C. Bentheimer plugs were selected with a homogeneous porosity profile (examples on figure 2), permeabilities ranging from 1.45D to 2D and porosities ranging from 20.5% to 22%. Note that the porosities here are obtained through image processing and represent the porosity that is directly visualized on 3D images. 97-99% of this porosity is connected and the rest made of disconnected porosity clusters is attributed to image processing uncertainties. This visualized porosity can be 1p.u to 3p.u less than the true porosity because it does not account the pore volume in clays which is under the resolution of the images. An experimental protocol exists to account for the sub-resolved porosity [13, 14] but in this case, we had access to almost the entire pore volume. It was then not necessary.

2.2. Fluids

We focus our study on oil/brine displacements. In order to be able to distinctly distinguish oil phase, brine phase and grains on 3D images, there is a need of a clear atomic density contrast between them. In our case, we doped brine with 7%wt of potassium iodide (KI) essentially.
Decane was used as mineral oil (**μ_D = 0.93cP, and ρ_D=0.73g.cc^{-1} at 25°C**). For ageing processes at 80°C to alter wettability, we replaced Decane with a dead oil [Dead oil A] with following characteristics: **μ_A = 6cP (2cP at 80°C), and ρ_A=0.845g.cc^{-1} at 25°C**.

2.3. Image acquisition and processing

3D images were acquired using a Zeiss Xradia Versa 520. Energy settings were chosen between 80kV and 100kV while power varied between 7W and 9W. Voxel size varied from 4µm for 4mm diameter plugs to 5µm for 1cm diameter plugs. Samples were analyzed on the total sample's length and we had to stitch a maximum of 9 segments (3cm length) which would take up to 22h in total acquisition time (~ 2h30 per segment).
Image processing was realized using Avizo 2020.3® and the open-source software ImageJ. Greyscale color code for the reconstructed data and Image processing sequences used are identical to the one used by Nono et al. [9].

2.4. Experimental set-ups

The cells designed in this study were used under same experimental conditions in terms of confining pressure, pore pressure and temperature during ageing if necessary. These parameters are fixed as follows: Confining pressure = 30 bars, Pore pressure = 10 bars and ageing temperature = 80°C. Different types of cells were developed for this study.

2.4.1. Oil flooding cell

Oil flooding experiments were achieved using the same set-up than that used by Berthet et al. [15], with end faces diffusers made of grooves. For this cell, samples were automatically 4mm diameter and almost 3cm length. The flow is achieved vertically, and the injections are started by respecting gravity direction. It means injecting the lighter fluid from top to bottom and the denser fluid from bottom to top. In this cell, the sample's end faces are in contact with only one flow line each. Pressure gradients are not measured at the rock end faces but on the flow lines outside the cell. A correction is made to take into account the pressure gradient they generate.

2.4.2. Porous-plate cells

We designed an in-house porous-plate cell with almost the same technical improvement as for Pentland et al. (2014) [16] enabling both the possibility to perform a porous plate experiment and to perform core flooding with flow

properties measurements (absolute/effective permeabilities). This cell entirely made of Peek® also enables 3D X-ray imaging for pore scale analysis. In these cells, samples are automatically 1cm diameter. The porous plate is made with a center hole enabling flooding. When the center hole is isolated, the flow is operated through the porous plate. During porous-plate experiments, oil invades the total volume of the center aperture at breakthrough because the capillary pressure there is lower than the capillary pressure needed to displace water in the porous-plate. Porous-plate experiments could also be achieved on the 4mm diameter plugs using the 4mm flooding cell described above (section 2.4.1). For this case, a full ceramic cylinder of 4mm diameter is placed between the sample's bottom face and the diffuser. No measurement of effective permeability is possible here because the ceramic is a full material without a center cylindrical aperture.

2.4.3. Centrifuge cell

At the very end, we also designed an in-house centrifuge cell enabling both the possibility to achieve centrifuge experiments and to acquire 3D X-ray images of the sample in it. With this cell, centrifuge experiments are performed under confining pressures. Samples used are automatically 1cm diameter.

In this way, the dry samples are initially loaded in the cell before any saturation and flooding steps. We avoid having the saturated plugs in contact with air or having to mount saturated plugs in jackets and air-filled cells which can increase the level of uncertainty on the experimental processes. By this way we also control the length of our samples and the end faces surface quality.

2.5. Experimental procedures

The overall experimental procedure is depicted in figure 4. The first part of the procedure (proc.1) aims to directly compare: porous plate (**PP**), centrifuge (**CF**) and oil flooding (**OF**) experiments during the first primary drainage for the same S_{wi} targeted. The overall procedure (proc.2) aims to investigate cleaning efficiency and its impact on primary drainage. In this paper, wettability assessment is achieved through ROS (remaining oil saturation) profiles. In this study, we focus on 14 samples in which 12 underwent only proc.1 while 2 samples underwent proc.2. The flowrates used in this study are reported in terms of capillary number (Ca) expressed in equation 1:

$$Ca = v.\mu/\gamma \qquad (1)$$

Where v represents the superficial fluid velocity ($m.s^{-1}$), μ the displacing phase viscosity ($P_a.s$) and γ the interfacial tension ($N.m^{-1}$).

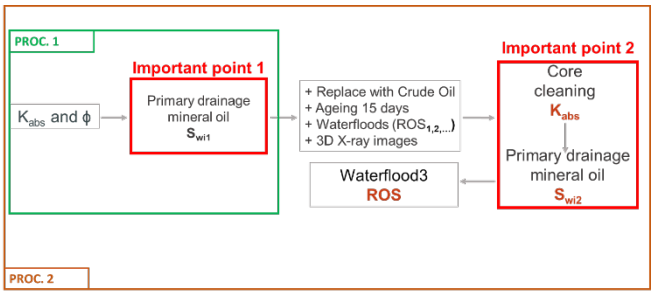

Figure 3. Experimental procedures used in this study. The green domain is proc.1 which aims in comparing first primary drainage data. Proc.2 (brown domain) starts with proc.1.

Proc.2 which includes proc.1 is performed as follows:

(i) Dry 3D scan of the whole sample mounted in the cell with a confining pressure of 30 bars, at 4 or 5 µm of voxel size (depending on the sample's diameter, respectively 4mm and 10mm diameter). Then the cell with the sample in it is moved from the micro-CT to the flooding stage.

(ii) Vacuum saturation and flushing at low rate (30µl/min) with 40 pores volumes (PVs) of brine with a pore pressure of 10 bars and a confining pressure of 40 bars. For the rest of the protocol, we maintained 30 bars of effective pressure. Measurement of the absolute permeability is achieved with rates varying from 10µl/min to 100µl/min (5 to 6 rates).

(iii) Primary drainage with Decane using either the porous plate (PP), the centrifuge (CF) or the oil flooding (OF) technique to target a known initial water saturation (S_{wi}). A multistep approach is used and corresponds to a gradual increase in capillary number for OF in unsteady-state mode, gradual increase in capillary pressure for PP and gradual increase in rotational speed for CF. Values of capillary number or capillary pressures or spinning rates depend on the target of initial water saturation. Here we monitor the DP for OF, the injecting syringe volume VS time for PP and the production for CF.

After the maximum rate/spin used, reverse the flow (only for CF and OF) using the maximum rate/spin to flatten saturation profiles. At the end of primary drainage, we perform a 3D scan of the whole sample and measure oil permeability at S_{wi} ($K_o(S_{wi})$). A close attention is done on measuring effective permeability especially when high S_{wi} values are targeted. We used oil flooding and 5 rates to measure effective permeability. For the OF method, the maximum rate used corresponds to a value less than the maximum rate used to achieve S_{wi}. For The PP method, we made sure that the pressure gradient during each oil flooding rate did not surpass the maximum capillary pressure implemented during the porous-plate displacement to achieve S_{wi}. Here, during the measurements we focused on how quick we obtained the plateau of gradient pressure for each rate and 2D X-ray projections of the outlet during permeability measurements. No brine was produced during these stages, and the pressure gradient stabilizations were fast. [**This is the end of proc.1**]

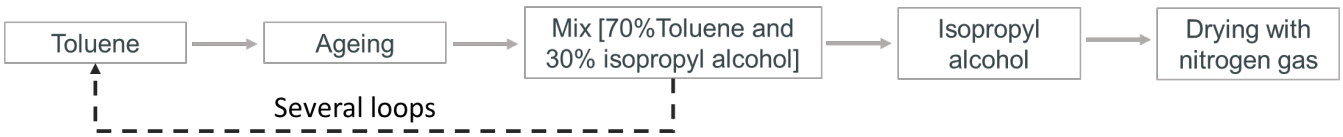

Figure 4. Classic cleaning sequence in core flooding laboratory

(iv) If ageing with crude oil is expected (only performed on 4mm diameter samples): replacement of the mineral oil with 5 PVs of toluene (at 10µl/min) then with 5 PVs of dead oil A (at 4µl/min) at 80°C in an oven to avoid wax appearance. Dynamic aging at very low rate (0.05µl/min) with dead oil A for 15 days. During ageing time, the flow is reversed after 7 days.

(v) After ageing, we perform a waterflooding of the sample at 50µl/min and 80°C till gradient pressure equilibrium then 3D scans of the sample at remaining oil saturation (ROS) and at 28°C which is the temperature of the micro-CT.

(vi) Sample cleaning: the cleaning process is depicted in figure 3. Two different approaches are tested: Cleaning at ambient temperature and cleaning at 80°C. The goal is to try to mimic an inefficient and an efficient cleaning. Cleaning consists in several loops, injecting toluene, then azeotropic mix of toluene and isopropyl alcohol (70%/30%) with an ageing time between both steps (in general 5 to 6 hours). When the sample is cleaned enough (colorless effluents), we inject 4 pore volumes of isopropyl alcohol and dry the sample using Nitrogen gas. The rate of injection is held constant at 40µl/min.

(vii) We restart the steps (i) to (iii) using exactly the same inputs (flowrates, pressures, injection time, time of reversal, etc.).

(viii) Waterflooding of the sample with brine and 3D scan to visualize fluids distribution. [**This is the end of proc.2**]

It is important to note that during all these steps (with OF, CF and PP methods) the plugs remained under confining and pore pressure in their initial cell from (i) to (viii).

To ease the reading of the paper and the identification of the samples we use the following formula for Bentheimer samples names:

B(a)-(b)-(c)(d) where: (a) stands for the protocol number (**1** for proc.1 and **2** for proc.2), (b) stands for the initial wettability (ww for water-wet and sw for alterated wettability using Surfasil®), (c) stands for the primary drainage method (PP: porous plate, CF: centrifuge or OF: oil flooding) and (d) stands for the number of the sample if there are many. An example of Bentheimer sample name can be: **B2-ww-CF3** meaning that this Bentheimer sample has undergone proc.2 with an initial water-wet wettability, using Centrifuge as main primary drainage method and is the third sample to undergo these steps.

The different plugs used with their geometry, porosity, permeability, average S_{wi} values, are given in Table 2. Due to the fact that our mini-plugs pore volumes were very smaller than the system dead volumes, we could not achieve a direct measurement of the produced volume. Material balance is achieved here by image processing on the part of the network that is visible. Image segmentation applied in this study is partly operator dependent. A variation of +/- 2% can be added as the variability of image segmentation.

Table 2. Bentheimer samples properties

		Sample name	Porosity µCT (%)	Perm. (D)	D (mm)	S_{wi} (%)	$K_{ro}(S_{wi})$
BENTHEIMER	Low S_{wi} targeted	B1-ww-OF1	21.3	1.53	3.92	7.5	0.84
		B1-ww-PP1	20.5	1.45	9.87	8	0.88
		B1-sw-OF1	21	1.7	3.92	35	0.1
		B1-sw-OF2	22	1.65	3.78	18.5	0.32
		B1-sw-PP	20.6	/	3.88	10.5	/
		B2-ww-OF1	20.5	2	3.85	5.3	0.75
		B2-ww-OF2	21.1	1.98	3.88	4	0.86
	High S_{wi} targeted	B1-ww-OF2	20.5	1.62	3.94	31	0.29
		B1-ww-OF3	21.5	1.68	3.85	47.5	0.22
		B1-ww-PP2	21	1.9	9.88	35.4	0.53
		B1-ww-CF	22	2.1	9.85		

3 Results and discussions

Results are divided into three topics:

i. Low targets of S_{wi}: In this section, we focused only on OF and PP methods. Experimental investigations are achieved on targets below 10% of initial water saturation. The same experimental inputs and chronology are used for each sample to target the same S_{wi}, disregarding wettability. For the OF method, a final capillary number of $Ca = 1.5x10^{-4}$ is used. For PP method, a maximum capillary pressure of $Pc = 100$ mbars was used.

ii. High targets of S_{wi}: In this section, high targets of S_{wi} are implemented. OF, PP and CF are used for Bentheimer. The maximum capillary number used during OF was $C_a = 1.5x10^{-5}$. For PP experiments, we used a maximum capillary pressure of $P_c = 35$ mbars and for the CF method, we achieved a single experiment using a spinning rate of 400rpm corresponding to an entry capillary pressure of 35 mbars.

iii. Cleaning efficiency impact: In this section, two Bentheimer samples underwent the overall proc.2 (figure 4) till the last waterflooding. As the two previous topics above will highlight the importance of wettability on S_{wi}, it is therefore mandatory to understand in which manner the wettability obtained after cleaning impacts our processes.

It is important to note that for low and high S_{wi}, effective permeabilities are measured using multi-rates injections of oil only. As shown by [9], disconnection of water and perturbations of the outlet water saturation occurred during primary drainage once oil breakthrough happened. These perturbations increase with rate and partly contribute to highly decreasing the actual outlet saturation and decreasing the impact of capillary end-effect on gradient pressure.

3.1. Low targets of S_{wi}

3.1.1. Low S_{wi} on water-wet porous media

Samples concerned: **B1-ww-OF1 and B1-ww-PP1 for proc.1, B2-ww-OF1 and B2-ww-OF2 for proc.2.**

We focus in this section on the first primary drainage. Everything that comes after the first primary drainage (B2's samples) will be discussed in the cleaning efficiency paragraph.

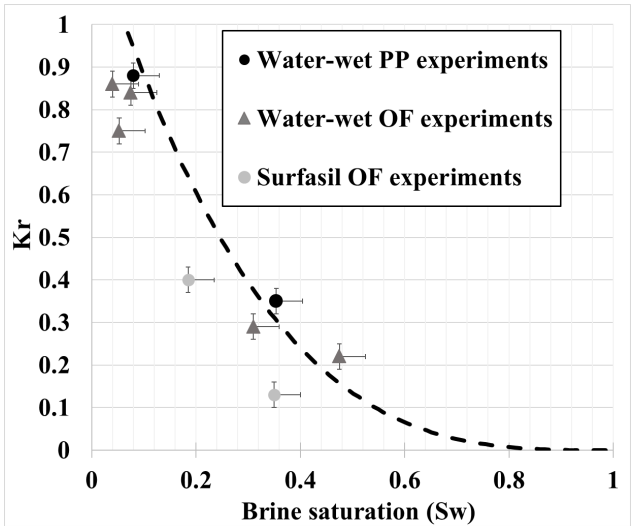

Figure 5. Synthesis of $K_{ro}(S_{wi})$ after primary drainage for low and high S_{wi}

Oil flooding experiments lasted ~ 2h to reach S_{wi} while the porous plate experiment lasted 3 days. In figure 5 we plotted primary drainage relative permeability values obtained at S_{wi} for all samples. We also plotted a Bentheimer sandstone primary drainage Kr curve taken from the literature [9] which is the result of a Corey fit of the experimental points reported in [19] and was successfully used for experiments on plugs [9] coming from the same batch as the samples used in this study.

Almost all the experimental values of oil relative permeability at low S_{wi} (from 4% to 8%) are close to the literature curve and no clear distinction can be made between each initialization method (figure 5) a part one OF point at S_{wi} = 5% with Kr_{ow} measured at 0.75 which is a bit below low S_{wi} cloud. Saturation profiles obtained by 3D image segmentation on each sample (figure 6) show homogeneous profiles without noticeable capillary end-effects while expected for water-wet porous media. Beyond the high Rapoport number used which reduces C.E.E, Nono et al. [9] also shown that the oil outlet saturation may increase with rate.

For both PP and OF, oil is connected from inlet to the outlet with 100% connectivity. At these low targets, brine remains in clays, corners, and films layers. No direct distinction at this stage is made between oil flooding and porous plate experiments at the macroscale based on the accessible pore scale observations made in this study. Both methods give similar results in terms of pore occupancy, oil global connectivity with reproducible values of S_{wi} and effective oil permeabilities. Based on Rucker et al. [11] we know that at the nanoscale, differences could arise regarding surface coverage and lead to different wettability after ageing. The authors observed for very close values of S_{wi} between CF and OF, very different wettability with the OF method being inefficient beside CF method.

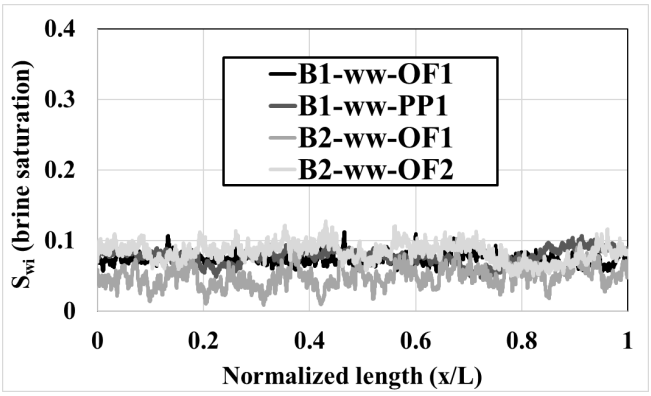

Figure 6. Saturation profiles for low targets of S_{wi} on Bentheimer

Regarding their conclusions, the CF method with high spinning rates to achieve low S_{wi} would have led to the same macro-scale observations on Bentheimer sandstones. Unfortunately, we could not access nanoscale properties and did not perform spontaneous displacements comparisons. As films layers are not visible due to the limits of the imaging set-up, we cannot draw the same conclusions of equity between the different methods at the nanoscale, specifically on surface coverage by films layers.

3.1.2. Low S_{wi} on non-water-wet porous media

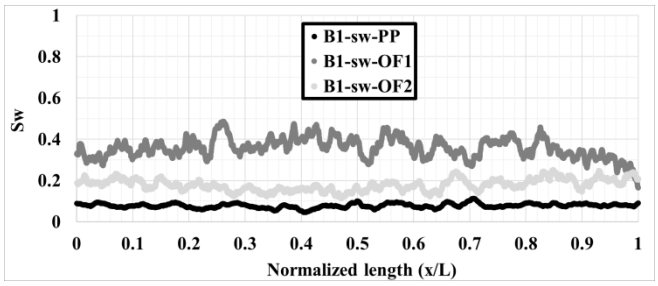

Figure 7. Water saturation profiles of surfasil-treated Bentheimer plugs, targeting low S_{wi}.

Samples concerned: **B1-sw-OF1, B1-sw-OF2, B1-sw-PP,.**

On **B1-sw-OF1 and B1-sw-PP**, oil flooding and porous-plate were performed respectively under the same conditions of capillary number and capillary pressure than that of water-wet Bentheimer plugs in section 3.1.1. On **figure 7** are plotted final saturation profiles. We observe a non-neglectable ~ 20-25 p.u higher average saturation for oil flooding (B1-sw-OF1) than water-wet samples but also with the porous-plate experiment at the same wettability. Both samples will be investigated distinctly.

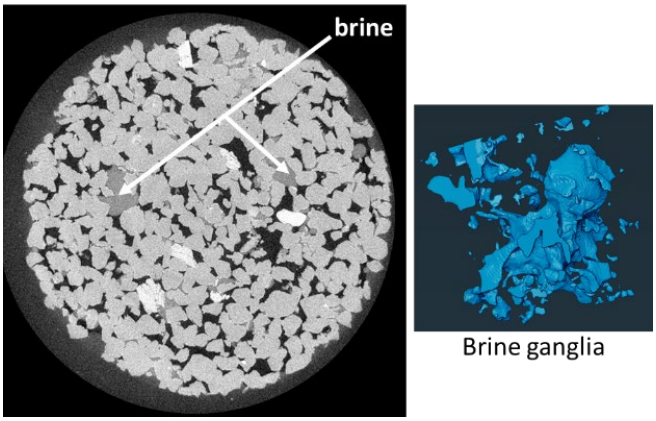

Figure 8. On the left: 2D slice of a Surfasil-treated Bentheimer at S_{wi}, on the right: isolated ganglia of brine

- ***B1-sw-OF1***: OF pore scale investigations on **B1-sw-OF1** highlight small pores and big pores filled with brine after oil flooding whereas for water-wet case, brine does not fill at all the big pores (figure 1, image (iii)). 3D segmentation shows big ganglia of brine connecting many pores and been surrounded and trapped by oil (figure 8). The geometries of ganglia highlight a clearly more oil-wet trend. Without dynamic imaging, we were not sure if snap-off could occur in these cases, but we believed trapping through snap-off of the brine phase should normally be very limited as there are no initial oil layers in the system. The sample is initially 100% brine saturated.

S_{wi} obtained on **B1-sw-OF1** being finally high, we could quantitatively compare the pore occupancy with a water-wet Bentheimer on which we achieved a high S_{wi} with close values. We choose **B1-ww-OF2** (Table 2) from which S_{wi} are close to each other (35% and 31%). To investigate pore occupancy, we used a pore network extraction code called GNextract developed with Imperial college of London [17] which was used to satisfactorily validate TotalEnergies' DRP workflow for multiphase flow simulation and relative permeability estimation against experimental core flooding experiments [18].

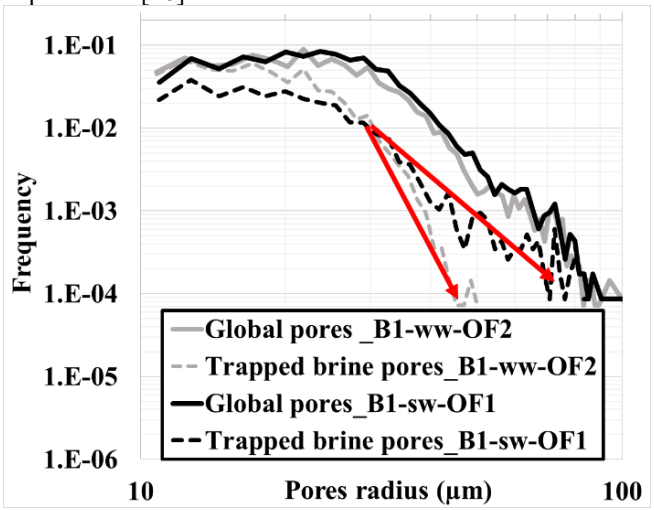

Figure 9. Comparison between water pore occupancy of a water-wet Bentheimer (B1-ww-OF2) and a Surfasil-treated Bentheimer (B1-sw-OF1) at same S_{wi}.

Results are depicted in figure 9. Continuous lines refer to total pores radius distribution and the dashed lines refer to distribution of pores radius in which at least 50% of brine is present.

Due to image segmentation uncertainties, we choose to remove all pores radius below 10µm so that the minimum pore diameter investigated is at least five times the pixel resolution (5x4µm = 20µm). We consider that this is the minimum size detectable by our segmentation process without large uncertainties. For both samples, we analyzed approximately the entire pore volumes. As expected, both samples exhibit the same total pore radius distribution curves confirming the good similar pore network of different Bentheimer plugs.

At S_{wi} for the water-wet case (grey color), there is 100% water in the smallest pores and the number of these pores decreases sharply when increasing pores radius. Above 50µm of radius, no more water pore exists. For surfasil-treated sample at S_{wi}, a higher fraction of small pores than the water wet case are filled with oil whereas the sample is initially 100% water saturated as the water-wet case. It means that oil displaced water in small pores and throats more easily than the water-wet case. When we increase in pores/throats radius, pores filled with water decrease but less quickly than the water-wet case. The contrast due to wettability is less abrupt than the water-wet case. At 30µm, there is a cross. The fraction of water pores become greater in the surfasil-treated case than in the water-wet case, till very big pores. There are larger pores/throats occupied by water for the surfasil-treated samples than the water-wet plugs.

Maximum water pores radius is around 90µm, almost 2 times higher than the water-wet case.

- ***B1-sw-OF2***: The experiment done on **B1-sw-OF1** was repeated on **B1-sw-OF2** but this time the maximum capillary number used was 4 times greater than the previous one. S_{wi} was decreased down to 18.5% but still remained 10p.u higher than water-wet cases at lower capillary numbers. On figure 10, we achieved pore occupancy comparisons between **B1-sw-OF2** and the water-wet case **B1-ww-OF2** (S_{wi} = 18.5% and S_{wi} = 31% respectively).

For the surfasil-treated sample (black color), some smallest pores are filled with oil. When pore radius increases, we observe a progressive and linear trend which is a decrease of water pores till ~ 30µm meaning that water mobilization affects all pores radius between 10µm and 30µm. Whereas for the water-wet case, the curvature confirms that the decrease is a function of size: big pores first before the small ones. After 37µm, Surfasil-treated curve (dashed black in figure 10) shows a sharp decrease, but the largest pore remains larger than the water-wet case (red circle in figure 10).

It confirms that even at moderate to lower water saturation, the pore occupancy dynamic remains affected, and the sequence of filling or trapping is totally different from a water-wet case. Lower targets of S_{wi} will be difficult to obtain in these cases because of the initial wettability.

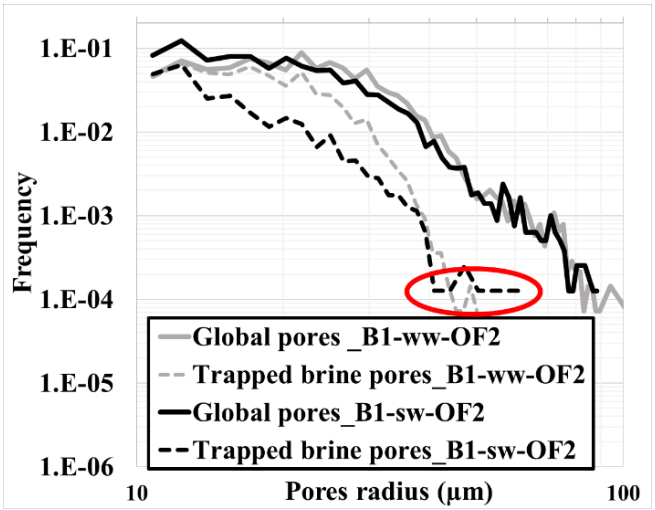

Figure 10. Comparison between water pore occupancy of a water-wet Bentheimer (B1-ww-OF2) and a Surfasil-treated Bentheimer (B1-sw-OF2).

To highlight the impact of this pore occupancy, we measured the effective permeabilities of oil for the surfasil treated samples for S_{wi}'s = 18% and 35% (figure 5).
The effective permeabilities calculated are clearly under the trend with differences up to 0.2 units. The oil phase network has its effective permeability reduced by the presence of water trapped in many big pores.

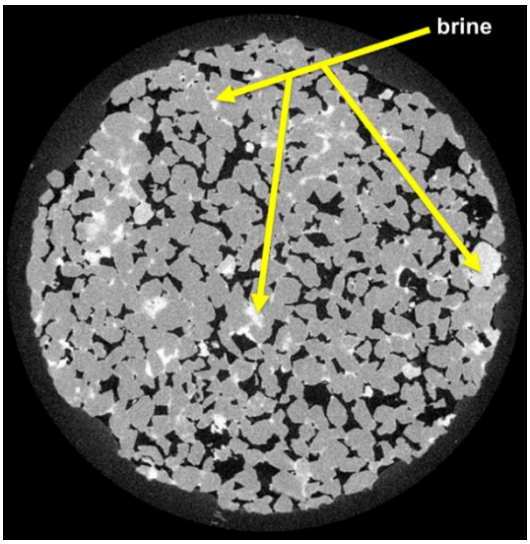

Figure 11. 2D slice of B1-sw-PP at S_{wi}. Water remains in small pores, crevices, corners, and clays.

- ***B1-sw-PP***: This experiment was achieved on a 4mm diameter plug without the possibility to measure effective permeability as the cell was not available. Porous plate primary drainage is operated in this case with a full porous plate without any center hole to measure flow properties. A highly doped brine was used in this case. The capillary pressure applied was 100 mbars as for the maximum capillary pressure applied on water-wet cases in section 3.1.1. Surprisingly, the S_{wi} obtained was low (figure 7), almost with same visual occupancy (figure 11) than the water-wet case. Water remained in clays and in very narrow pores. If the system is completely oil-wet, we expect the filling sequence to be reversed with oil filling preferentially the small pores before the big pores and we expect to see disconnected blobs of brine trapped in some big pores as we observed on B1-sw-OF1. The results obtained then raised some questions:

(i) Does the surfasil treatment in this case was not done properly? – Samples were prepared through a series of batches. The Surfasil-treated samples used in this study come from the same batch. The probability that this sample followed a process different from the others is very low regarding waterflooding results on which the observations made were similar to what observed on figure 1 for surfasil treated samples.

(ii) Is there a difference between the trapping occurring during OF and PP? – Trapping may differ. For a water-wet case, at high pressures, S_{wi} is finished to be achieved by films drainage no matter if we are performing OF or PP method. High pressures will always lead to decrease S_{wi} as water layers remain connected. For a non-water-wet case, no initial layer flow is available to decrease S_{wi} with increasing pressure. In addition, the frontal invasion evolves with a constant pressure during PP method whereas it varies for the OF method meaning the invasion patterns could differ and so could be the trapping behind the front. The OF capillary pressure distribution is not homogeneous at S_{wi} whereas PP capillary distribution is.

(iii) Wettability obtained with surfasil treatment is close to an intermediate wettability? – If the system is neutral wet ($\theta \sim 90°$), water production is maximized at breakthrough during primary drainage as capillary forces are very low and very low S_{wi} value is expected. But it should also be the case during oil flooding. We observed that it is not (figure 1).
Further investigations are needed on this topic. The next step will be to observe the filling sequence at the pore scale through X-ray imaging of the intermediate equilibrium capillary pressures stages.

3.2. High targets of S_{wi}

3.2.1. High S_{wi} on water-wet porous media

Samples concerned: **B1-ww-OF2, B1-ww-OF3, B1-ww-PP2 and B2-ww-CF.**
In this section capillary end-effects (C.E.E) are expected to be the main issue to cope with. For OF and CF experiments,

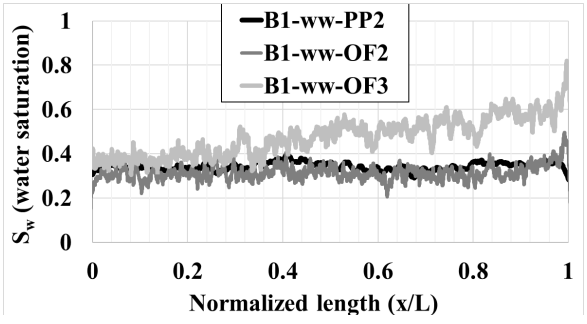

Figure 12. Saturation profiles of water-wet Bentheimer samples at the end of primary drainage (after reversals), targeting high S_{wi}

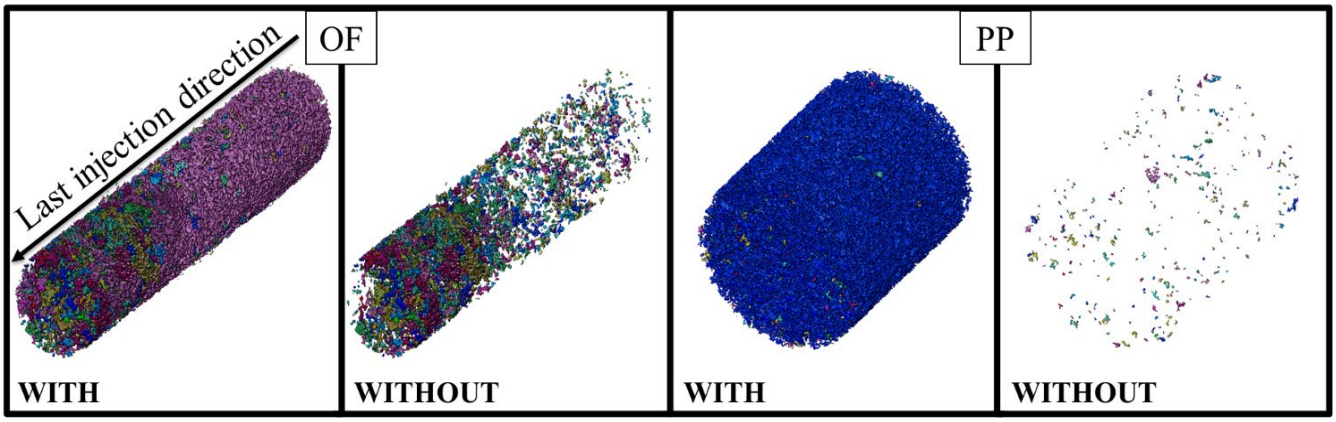

Figure 13. Example of oil disconnected clusters after primary drainage with and without the percolating cluster. We observe less disconnected and well distributed clusters for the PP method and the opposite for the OF method (**B1-ww-OF2** and **B1-ww-PP2**)

reversal flooding and spinning were achieved to flatten saturation profiles impacted by C.E.E. Effective permeabilities at S_{wi} on PP and OF experiments are available.

For the CF experiment, due to its latest arrival into the experimental pipe, we just achieved a quick test to confirm the dynamic and crucial observations that were observed especially during the OF experiment. Thus, saturation profiles which are reported on figure 12 do not concern CF experiment. As expected, for OF profiles, we observe gradients of saturation, especially near the outlet end face of plugs even after reversal flows. PP gives very homogeneous results.

Despite saturation gradients, the $K_o(S_{wi})$ reported on figure 5 are in a cloud which is near the literature curve. Capillary end-effect should normally highly impact effective permeabilities, and more when the sample is so permeable [9, 20]. A lot more experiments must be achieved to be able to detect a trend.

The crucial differences come from pore scale investigations. 3D images at S_{wi} were segmented and oil total volume was isolated. We observed a lot of disconnected oil clusters for samples gone under OF method. The principal oil cluster is connected from the inlet to the outlet, but the fraction of the disconnected clusters which are not taking part to the flow varied from 5% (very flat saturation profiles with little C.E.E as **B1-ww-OF2**) to almost 15% of the total oil volume (high saturation gradient as **B1-ww-OF3**) whereas the PP method gave a maximum of 0.1% of disconnected cluster mainly ascribed to segmentation uncertainties. For example, on figure 13, we show an entire OF sample and an entire PP sample with and without the percolating cluster. Each colored cluster is a disconnected cluster. When capillary end-effect is involved, a lot of clusters are disconnected because of the reversal flow. This is due to the brine held at the outlet by C.E.E which is being re-injected back-into the sample through oil injection from outlet to inlet. From a water-wet perspective, this causes a partial imbibition process with trapping of an important amount of oil. Afterwards, the pressure needed to access pores where there is trapped oil and reconnect these disconnected clusters will be higher than if no oil phase was trapped in these pores. Another observation is made on the clusters size. In figure 14, we plotted clusters size (total volume in µl) in function of their center of geometry on B1-ww-OF2.

In this graph, we do not represent the percolating cluster. We observe a general increasing trend of cluster size (red ellipse) when we go from inlet to outlet. Larger clusters are found near the outlet. This could be due to the decrease of capillary pressure towards the outlet end of the sample which causes disconnection of larger oil clusters during the re-imbibition process, on a few throats by snap-off or cooperative pore filling.

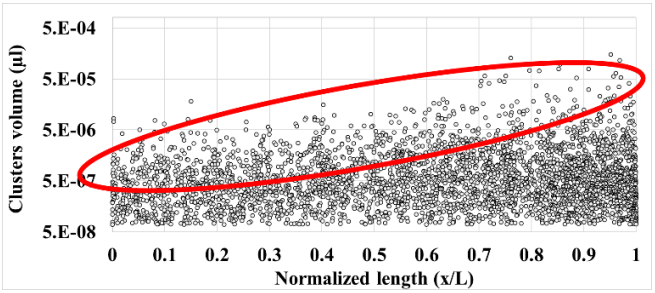

Figure 14. Disconnected oil clusters size distribution

A quick test was achieved with the CF cell and a small length plug (1cm) to confirm that this disconnection also happens on CF method when we do reverse the flow in the sample. Before the reverse, we will consider for the CF method that the drainage is done from the "first inlet" to the "first outlet". Then when afterwards we turn the sample into the CF device to reverse the drainage, we consider that we go from the "last inlet" to the "last outlet". Last inlet is the same location as the first outlet and last outlet is the same location as the first inlet. Without measuring multiphase flow properties, we first performed a quick primary drainage at low spinning rate to keep a large brine saturation at the outlet. Then, before the end of primary drainage we returned the sample and achieved another quick primary drainage at the same rate. We wanted to observe if:

(i) The first inlet (which is the last outlet) had a lot of disconnected clusters?

(ii) The last inlet had more connected clusters?

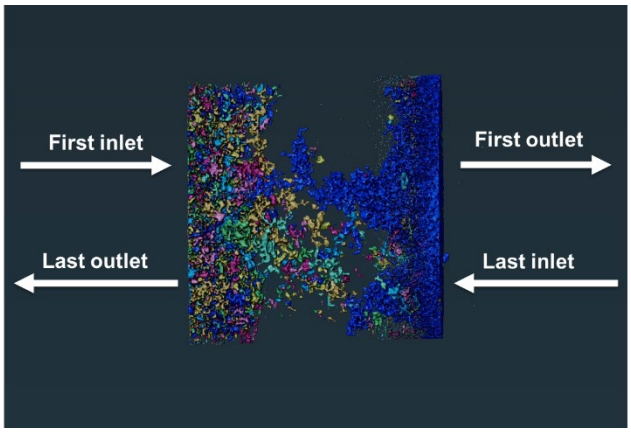

Figure 15. Clusters distribution at the end of the CF experiment. Each disconnected oil cluster has a different color.

In figure 15, we show oil clusters distribution at the end of the CF experiment. We observe a large cluster (blue) at the last inlet which is oil re-invading the pores from drainage process. This cluster seems connected with very few disconnected clusters around. Initially, as it was the first outlet, there was a high saturation of brine.
At the opposite, we observe a lot of disconnected oil cluster at the last outlet which was the first inlet before the reverse spinning. The oil that invaded initially this first inlet was then connected as the blue cluster. Because of the reverse spinning, the displacement of brine from the capillary end-effect zone to the inlet generated trapping of oil. With this quick experiment, it is now evidenced that the trapping observed is mainly due to re-imbibition processes and not image analysis uncertainties or something else.
For OF and CF, there can be a non-neglectable number of disconnected clusters at the end of flooding or spinning even if the saturation profiles seem flat after reversals. These disconnected oil clusters have a good probability to not be reconnected during replacements with crude oil or after ageing. Thus, the wettability in these pores after ageing may be different from the other pores crossed by the percolating cluster.
The variation of clusters size towards the outlet can affect wettability homogeneity within the sample. Despite a flat saturation profile, the disconnected oil acts apart from the principal channel of flow. In this case, wettability may be well altered at the inlet and less at the outlet.

3.3. Cleaning efficiency impact

Samples concerned: **B2-ww-OF1 and B2-ww-OF2**

In this section we choose two samples that underwent the overall proc.2. Ageing achieved with crude oil changed the wettability of the plugs from water-wet to weakly water-wet or mixed-wet behaviour. An example of ROS profile is depicted in figure 16. The ROS was around 20% while for water wet Bentheimer sandstone, residual oil saturation is around 30% to 45% [9]. We also could clearly identify a slight capillary end effect to oil near the outlet which confirms that the wettability of the samples was altered using dead oil A.

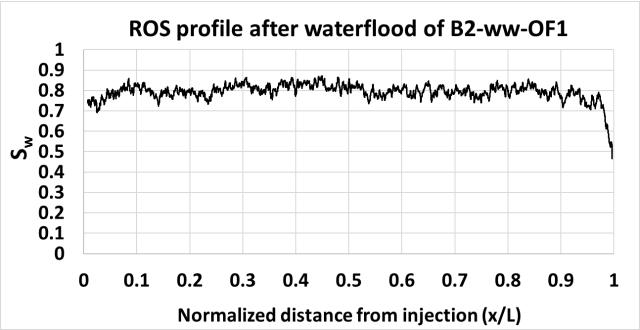

Figure 16: ROS profile obtained after the first waterflooding of B2-ww-OF1 following 2 weeks of ageing with dead oil A.

The only difference between the two samples used in this section is that **B2-ww-OF1** was cleaned using only one loop (figure 3) and **B2-ww-OF2** was cleaned with a multi-loop process. The goal is to compare the two primary drainages: before and after cleaning, which are performed using identical flooding conditions.
In table 3, we reported experimental properties measured on both samples during proc.2.

Table 3. Properties measured on Bentheimer samples during proc.2 achievement.

Sample name	K_w before cleaning (D)	S_{wi} before cleaning (%)	S_{wi} after cleaning (%)	K_w after cleaning (D)
B2-ww-OF1	2	5.3	10.6	1.4
B2-ww-OF2	1.98	4	22	1

We do observe a reproducible increase of S_{wi} after cleaning despite identical capillary numbers and pore volumes injected to the initial primary drainage before cleaning and a reproducible decrease of absolute permeability after cleaning.
An illustration of this increase is presented on a 2D slice of B2-ww-OF1 in figure 17. We observe that in general, the increase of S_{wi} is principally located in very narrow pores.

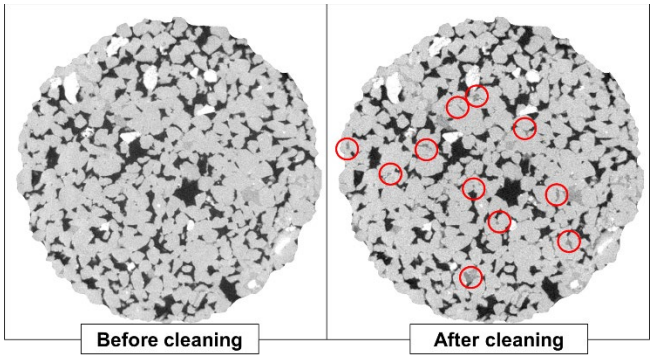

Figure 17. Comparisons of 2D slice at S_{wi} before cleaning and After cleaning of B2-ww-OF1

We also observed an important reproducible decrease of permeability after cleaning, which can lead to almost 50% loss of absolute permeability without any observable change on 3D images. Additional experimental investigations showed that this decrease happens when the mix of the two solvents (Toluene and isopropyl alcohol) is injected into the samples. The physical reasons are not yet understood and

are still under investigations but if the pore-network is conserved, then the issue is probably under resolution thus maybe in clays.

Regarding these results, we had two possibilities of explanations:

(i) The increase of S_{wi} after cleaning is not linked with the loss of permeability: then it means that despite the cleaning, the final wettability may not come back to its initial state. We could be in presence of a weakly water-wet pore network with less strongly water-wet pores thus water trapped in more and more narrow to intermediate pores-throats sizes.

(ii) The increase of S_{wi} after cleaning is linked with the loss of permeability: which is also likely to happen as at constant wettability, a loss of permeability increases the displacement pressure needed to invade pores (capillary forces). As we used the identical protocol of primary drainage before cleaning, we can only reach higher values of S_{wi} as viscous forces are not enough to counterbalance this increase in capillary forces.

4 Conclusions

This paper presents a detailed analysis at the pore-scale of different methods to achieve S_{wi} considering wettability. Bentheimer sandstone was used with different initial wettability.
What lessons can be learned about this experimental investigation?

- The porous plate method remains the most robust technique at almost all points of view. The only drawback is about the time needed to achieve an experiment.
- For low S_{wi} on water-wet plugs, we observe no distinction on fluids connectivity, pore occupancy and no capillary end effects between these initialization methods. However, a special caution must be required for the OF method. As shown by Rücker et al. [11, 12], clear distinctions can arise at the nanoscale on surface coverage. The lack of capillary pressure and the trend to bypass parts of the pore network for the OF method decreases the capacity to change wettability than the CF and the PP methods where we have control of the applied capillary pressure thus the invaded pore/throat sizes. When possible, one should clearly privilege PP method as it maintains a constant capillary pressure through the sample's length. It has the advantage that it can be used for short or long cores, in jackets with pore pressures and at temperature. It is directly adapted for oil flooding set-ups. Some systems also exist coupling the PP method with flooding experiments [16]. If not possible, it is generally better to rely on the CF method to achieve S_{wi}. The main advantage of CF regarding OF is that we avoid bypassing pore network structures and control the real capillary pressure versus length applied on the sample. Controlling capillary pressure distribution is a real advantage as one can size the threshold pressure which can counter-balance sufficiently the water films disjoining pressure so as to much better alter wettability. However, CF also suffers of capillary end-effects and there are some important constraints such as the samples length which is limited, the experimental pressure and temperature which is most of the time at ambient conditions and the sample handling. Therefore, the coupling between PP and OF may be the best option taking into account all different constraints.
- For non-water-wet plugs, a conclusion is quite difficult to draw. According to our results that are to be confirmed with a lot more experiments, low initial water saturation is achieved with the porous plate method. We observed different sequence of trapping which may be due to the invasion patterns difference between methods. Oil flooding technique generates a lot of disconnected water clusters with a lower oil effective permeability. The pore occupancy (brine in large pores) is different from what is wanted.
- When targeting high S_{wi} (i.e. transition zone) on water-wet plugs, we must deal with capillary end-effect linked to a gradient of capillary pressure on the sample's length. It affects essentially OF and CF methods. If no porous plate is used then we should at least find a way to avoid saturation gradients, disconnecting oil clusters and more over homogenize water film thickness in the overall volume. As it is shown in this study, without optimized set-ups (coupling of OF and PP [16] for example) it is clearly impossible to avoid trapping when achieving reversals. But we can try to decrease its impact. Some ways forward to investigate can be suggested: (i) the first suggestion would be to start reversing the flow after the maximum capillary (OF) or bond number (CF) to be used for unidirectional injection. We can expect that it limits the water volume held at the outlet (C.E.E) that will be re-injected in the sample and the reverse will act to thicken the large water films left near the outlet volume because of the capillary end effect. (ii) the second suggestion which should come after achieving the first one would be to perform several reversals at maximum capillary and bond number to avoid heterogeneity in terms of clusters size towards sample's length for the disconnected clusters. The goal here would be to reconnect the maximum of possible clusters to the principal percolating oil cluster and to homogenize disconnected clusters sizes towards the sample's length. Then a nano-scale study of surface coverage as done by [11, 12] has to be achieved to clarify whether these reversals help to homogenize the potential of having wettability altered through the overall length of the sample.

We thank TotalEnergies for their financial support and the permission to publish this paper. We also acknowledge Dr. M. Regaieg, Dr. F. Pairoys, Mr Q. Danielczick, Mr R. Brugidou and Mr M. Bizeau for their insightful discussions and contributions.

References

1. Z. Zubo, L. Manli and C. Weifeng, “An Experimental Study of Irreducible Water Saturation Establishment”, International Symposium of Core Analysts, Avignon, France, 2014 [SCA2014-070]
2. M. Fleury, “The spinning porous plate (SPP) method: a new technique for setting irreducible water saturation on core samples”, International Symposium of Core Analysts, Noordwijk, Netherlands, 2009 [SCA2009-08]
3. C. McPhee, J. Reed and I. Zubizarreta, “Core analysis: a best practice guide”, Amsterdam: Elsevier, 2015.
4. R. Farokhpoor, L. Sundal, A. Skjaerstein, A. Hebing, X. Zhang and L. Pirlea, “Core cleaning and wettability restoration – selecting appropriate method”, International Symposium of Core Analysts, 2021 [SCA2021-016]
5. O. Vizika, J.P. Duquerroix, “Gas injection and Heterogeneous Wettability: what is the relevant information that petrophysics can provide”, International Symposium of Core Analysts, Calgary, Canada, 1997 [SCA-9708].
6. C. J. Landry, Z. T. Karpyn and M. Piri, (2011). Pore-scale analysis of trapped immiscible fluid structures and fluid interfacial areas in oil-wet and water-wet bead packs. Geofluids, 11(2), 209-227. https://doi.org/10.1111/j.1468-8123.2011.00333.xF. De Lillo, F. Cecconi, G. Lacorata, A. Vulpiani, EPL, **84** (2008).
7. C.A. McPhee, and K.G. Arthur. "Relative Permeability Measurements: An Inter-Laboratory Comparison." Paper presented at the European Petroleum Conference, London, United Kingdom, October 1994. doi: https://doi.org/10.2118/28826-MSC.A.McPhee & K.G.Arthur SPE 28826 October 25-27 1994.
8. Wilson O.B., Tjetland B.G. and Skauge A., “Porous plates influence on effective drainage rates in capillary pressure experiments”, International Symposium of Core Analysts, Edinburg, Scotland 2001 [SCA2001-30].
9. F. Nono, P. Moonen, H. Berthet and R. Rivenq, “Multiphase flow imaging through X-ray microtomography: Reconsideration of capillary end-effects and boundary conditions”, International Symposium of Core Analysts, Pau, France 2019 [SCA2019-019].
10. F. Pairoys, C. Caubit, M. Alexander and J. Ramos, “Comparing Centrifuge, Steady-State and Semi-Dynamic methods for relative permeability and capillary pressure determination: New Insights”, International Symposium of Core Analysts, Online, 2021 [SCA2021-019].
11. M. Ruecker, W.-B. Bartels, G. Garfi, M. Shams, T. Bultreys, M. Boone, S. Pieterse, G. C. Maitland, S. Krevor, V. Cnudde, H. Mahani, S. Berg, A. Georgiadis, P. F. Luckham, Relationship between Wetting and Capillary Pressure in a Crude Oil/Brine/rock system: From Nanoscale to Core-Scale Journal of Colloid and Interface Science 562(7), 159-169, 2020.
12. M. Rücker, W.-B. Bartels, T. Bultreys, M. Boone, K. Singh, G. Garfi, A. Scanziani, C. Spurin, S. Yesufu, S. Krevor, M. J. Blunt, O. Wilson, H. Mahani, V.Cnudde, P. F. Luckham, A. Georgiadis and S. Berg, “Workflow for upscaling wettability from the nano- to core-scales”, International Symposium of the Society of Core Analysts, Pau, France, 2019 [SCA2019-07]
13. Q. Lin, Y. Al-khulaifi, B. Bijeljic and M.J. Blunt, (2016). Quantification of sub-resolution porosity in carbonate rocks by applying high-salinity contrast brine using X-ray microtomography differential imaging. Advances in Water Resources. 96. 10.1016/j.advwatres.2016.08.002.A. Mecke, I. Lee, J.R. Baker jr., M.M. Banaszak Holl, B.G. Orr, Eur. Phys. J. E **14**, 7 (2004)
14. Q. Lin, B. Bijeljic, H. Rieke and M. J. Blunt, (2017). Visualization and quantification of capillary drainage in pore space of laminated sandstone by a porous plate method using differential imaging X-ray micro-tomography. Water Resources Research, 53, 7457–7468. https://doi.org/ 10.1002/2017WR021083
15. H. Berthet, P. Andriamananjaona, S. Barbouteau, M. Hebert, R. Farwati, R. Meftah, G. Quenault, J.P. Chaulet, , R. Brugidou, and R. Rivenq, “Capillary desaturation curves and insights on trapped oil at the pore-scale, in water-wet and oil-wet sandstones,” International Symposium of the Society of Core Analysts, SCA2018 Trondheim, Norway, (2018) [SCA2018-036].
16. C.H. Pentland, R.M. El-Maghraby, S. Iglauer and M.J. Blunt, “The toroidal porous plate: A new method to facilitate waterflooding”, International Symposium of the Society of Core Analysts, SCA2014, Avignon, France 2014 [SCA2014-068].
17. A.G. Raeini, B. Bijeljic, M.J. Blunt: Generalized network modeling of capillary-dominated two-phase flow. Physical review.E97(2-1), 23308 (2018). Doi:10.1103/PhysRevE.97.023308F. De Lillo, F. Cecconi, G. Lacorata, A. Vulpiani, EPL, **84** (2008)
18. M. Regaieg, I. Bondino, C. Varloteaux, T.F. Faisal, J. Yang and R. Rivenq, “Large two phase Digital Rock Physics simulations for relative permeability uncertainty assessment”, International Symposium of the Society of Core Analysts, SCA 2021, Online, [SCA2021-007].
19. M.J. Blunt, “Multiphase Flow in Permeable Media: A Pore-Scale Perspective,” Cambridge University Press. doi: 10.1017/9781316145098, 2017
20. S.K. Masalmeh, “ Impact of capillary forces on residual oil saturation and flooding experiments for mixed to oil-wet carbonate reservoirs”, International Symposium of the Society of Core Analysts, Aberdeen, Scotland, 2012 [SCA2012-11].